RESEARCH

Lawsone and Lavender Oil Incorporated Nanostructured Lipid Carriers: A Sustained Delivery Platform for Full-Thickness Wound Healing

Sara Daneshmand[1] · Ali Tahani[1] · Meysam Saberi[1] · Omolbanin Shahraki[2,3] · Jafar Shahraki[4]

Abstract

Lawsone, a naphthoquinone phytochemical compound present in the plants such as henna, was found to increase the healing process. However, clinical applications are impeded owing to the poor water solubility, low bioavailability, and dyeing property to the hair and skin. Nanostructured lipid carriers (NLCs) are appropriate carriers that cover undesirable effects of drugs, afford sustained release over a prolonged period of time, reduce systematic effects, decrease irritation, and increase tolerance. In this research, a formulation of lawsone incorporated NLC was prepared, and characterized for pharmaceutical application. The synthesized formulation was characterized using electron microscopy, polydispersity index, and zeta potential, and entrapment efficiency and malondialdehyde (MDA) level were evaluated. In order to assess wound healing potential, the wound area was measured at different times post-treatment, showing a structured tissue with better healing signs in NLC- L_w- L_v group in comparison with alpha ointment. NLC- L_w- L_v (NLC containing lawsone and lavender) formulation with mean size of 165.3 ± 4.2 nm, polydispersity index of 0.211, zeta potential of -24.3 mV, and entrapment efficiency of 79.3 ± 2.9 was subjected to further experiments as optimized formulation. The ex vivo evaluation of formulation in mouse skin indicated better retention, less residue, and permeation in comparison with alpha ointment as standard. MDA level, as the indicator of lipid peroxidation, was lower in the NLC- L_w- L_v treated group. Histological score of microscopic wound healing parameters, such as swelling, re-epithelialization, formation of fibrotic tissue, and granulation, presented significantly better wound contraction in NLC- L_w- L_v treated group. In conclusion, our results propose the effective wound healing ability of lawsone, proved by more effective and an earlier stimulation of wound contraction.

Keywords Nanostructured lipid carriers · Lawsone · Lavender · Response surface method · Wound healing

✉ Omolbanin Shahraki
o.shahraki@gmail.com

✉ Jafar Shahraki
jafar.shahraki@gmail.com

1 Department of Pharmaceutics, Faculty of Pharmacy, Zabol University of Medical Sciences, Zabol, Iran

2 Pharmacology Research Center, Zahedan University of Medical Sciences, Zahedan, Iran

3 Cellular and Molecular Research Center, Research Institute of Cellular and Molecular Sciences in Infectious Diseases, Zahedan University of Medical Sciences, Zahedan, Iran

4 Department of Pharmacology and Toxicology, Faculty of Pharmacy, Zabol University of Medical Sciences, Postal Code, Zabol 98616-15881, Iran

1 Introduction

The skin is defined as an immunologic barrier against pathogens and external harms that regulates the moist and temperature. Some skin damages such as chronic wounds and deep burns are very difficult to treat [1]. Despite different attempts for developing effective treatments, the outcomes have been unsatisfactory. The successful strategies are expected to rapidly restore acute and chronic wounds and also improve the quality of wound healing in patients. Wounds can be classified into two categories: acute wounds that are caused as a result of physical damage and exposure to intense irradiation, heat, and corrosive compounds. Under suitable condition, the acute wounds heal in a relatively short period of time. Chronic wounds appear in the case of diseases such as diabetes and healing occur in a longer time, unless the disease origin is recognized [2, 3].

There has been a substantial amount of focus in recent years on the investigation of the mechanism through which

herbal medicines and pure natural products contribute to the process of wound healing in recent years. It appears that certain herbal medicines possess the ability to exert their wound healing effect through different mechanisms and display their curative attributes at different stages of the wound healing process. Flavonoids, anthraquinones, and naphthoquinones demonstrate a remarkable capacity to exhibit wound healing activity [4, 5].

Lawsonia inermis, typically named as Henna, is a medicinal plant widely found in southern part of Asia, i.e., India, Bangladesh, and Iran. Lawsone is a phytochemical compound bearing naphthoquinone structure, that is extracted from the dried powdered leaves of henna [6]. This class of natural aromatic compounds has been identified for their dyeing properties.

Lawson binds to keratin, causing an orange red color on skin and hair. In addition to staining, a variety of pharmacological activities have been reported for lawsone such as antibacterial, antifungal, antiparasitic, tuberculostatic, analgesic, anti-inflammation, cytotoxic, nematicid, anticoagulant, anti-hair loss, increasing wound healing rate, antioxidant, and angiogenesis activity, burn and chronic wound treatments [7, 8].

In a reported research, electrospun nanofibers were developed that caused sustain release of lawsone during a 20-day period and induced wound healing and significantly increased cell attachment and proliferation [9]. In another study, ethanolic extract of henna leaves was confirmed as oral or topical ointment for wound healing [10]. Lakshmi et al. prepared a topical lawsone gel using Tara gum and HPMC K15M by dispersion process that was tested in the excision wound model showing that the wound healing ability of formulation is significantly more than the control [11] ($P < 0.05$). Another in vivo experiment was performed to evaluate the wound healing capacity of gels and films based on cuttlefish skin gelatin, combined with aqueous henna extract. The formulation enhanced healing activity, prevented inflammation damages, improved antioxidant enzymatic effects, and decreased MDA content [12].

Despite valuable pharmacological activities, the application of lawsone is limited due to dyeing property to hair and skin, poor solubility, and low bioavailability.

Another medicinal plant with wound healing activity, *Lavandula spica* L., is an evergreen shrub of Lamiaceae family cultivated in the Mediterranean countries [13]. Essential oil of lavender is used for the preparation of bactericidal Livian and Lavandic alcohol [14]. Other valuable pharmacological characteristics such as sedative, anti-inflammatory, analgesic, antidepressant, antibacterial, and antifungal properties have been mentioned. Also, lavender can effectively heal wounds and burns [15].

The effect of lavender on wound healing has been discussed in several investigations including human trials and in vivo and in vitro models [16, 17]. The healing ability of lavender was revealed in 1910. The molecular mechanism of topical lavender essential oil in the healing process via acceleration of granulation, tissue remodeling, and increasing the differentiation of fibroblasts through TGF-β was revealed by Mori et al. [18]. The effect of lavender on chronic ulcers [19], oral mucosal wounds [20], gynecologic wound healing [21], postepisiotomy pain, and REEDA scores [22] were clinically evaluated.

The biological effects of the essential oils may diminish or get lost as a result of instability in exposure to light, air, and heat. Then, it is necessary to improve their availability and biological properties through nanotechnology approaches that also enables sustained and site-specific delivery. A successful nano-scale delivery system is able to penetrate through various barriers such as skin, releases the drug content in a controlled manner, and is stable in nanometer range. Nanostructured lipid carriers (NLCs) are one of the promising delivery approaches. NLCs represent distinctive characteristics such as small particle size, large surface area, and drug loading capacity [23].

NLCs represent an advanced formulation of solid-lipid nanoparticles (SLNs), which belongs to the category of lipid-based drug carriers. In comparison to SLNs, NLCs exhibit a composition comprising both solid and liquid lipids, thereby facilitating an augmentation in drug loading capacity and the avoidance of initial burst release [24, 25]. Recently, there are some reports on the utilization of NLCs as carriers for drug delivery to specific areas through various methods of administration. An example of this is the widespread use of NLCs in cosmetics and dermatological applications for the purpose of topical delivery [26, 27].

In this study, nano size NLCs of lawsone were prepared to shelter the orange red color to exert the pharmacological properties in wound healing, and lavender oil as the liquid lipid with wound healing properties was applied in the formulation. The best formulation was characterized in terms of size, morphology, encapsulation efficiency, drug content release, and penetration. In vivo and ex vivo, histopathological tests were performed in mouse models, confirming that the formulation containing both lawsone and lavender is an effective treatment for wounds.

2 Materials and Methods

2.1 Materials

Tween-20 (polysorbat), Span® 80, and Stearic acid were purchased from Merck Company (Germany). Lawsone was obtained from Golexir Pars Co. (purity ≥ 95%). DMSO was provided from Dae Joung (Korea). Lavender oil was from Barij Essence (Iran). Ketamine and xylazine were provided

Table 1 Design of experiments by central composite design (CCD) for optimization of parameters

Run	A:lipid w/w%	[a]Lipid ratio	C:surfactant w/w%	[b]D:feed ratio of surfactant%	Lawsone w/w%	Average size (nm)±SD	Zeta potential (mV)±SD	Polydispersity±SD
1	4.00	4.00	2.00	1.25	0.1	322±4.25	−22.1±7.12	0.371±0.051
2	4.00	4.00	2.00	1.25	0.06	335±6.25	−21.3±6.78	0.381±0.025
3	4.00	4.00	2.00	1.25	0.02	321±5.32	−22.8±5.32	0.360±0.078
4	4.00	4.00	2.00	1.25	0.06	338±3.71	−21.3±6.87	0.375±0.038
5	4.00	4.00	3.00	1.25	0.06	295±6.52	−22.3±7.15	0. 291±0.042
6	3.00	4.00	2.00	1.25	0.06	201±8.27	−21.2±8.37	0.260±0.038
7	4.00	3.00	2.00	1.25	0.06	298±7.34	−23.1±5.32	0.302±0.046
8	4.00	4.00	2.00	0.5	0.06	322±6.73	−22.7±4.33	0.361±0.071
9	5.00	5.00	1	2	0.02	462.1±5.81	−20.1±2.17	0.512±0.058
10	4.00	5.00	2	1.25	0.06	362±1.13	−23.2±3.14	0.372±0.087
11	4.00	4.00	2	2	0.06	358±2.85	−23.8±7.20	0.369±0.052
12	3.00	5.00	3	2	0.02	165±2.91	−24.3±3.25	0.211±0.043
13	5.00	5.00	3	0.50	0.02	432±2.35	−23.2±9.18	0.460±0.059
14	3.00	5.00	1.00	2	0.1	223±9.75	−24.2±3.35	0.271±0.068
15	4.00	4.00	2	1.25	0.06	331±5.82	−22.9±5.41	0.362±0.028
16	5.00	3.00	1	2	0.1	443±4.6	−21.2±4.70	0.482±0.085
17	5.00	5.00	1	0.50	0.1	451±3.21	−23.2±5.38	0.0473±0.025
18	3.00	3.00	1	0.50	0.02	192±5.29	−22.1±7.18	0.438±0.063
19	4.00	4.00	2	1.25	0.06	338±7.54	−21.2±7.90	0.365±0.081
20	3.00	5.00	3	0.50	0.1	182±5.28	−23.7±6.81	0.275±0.079
21	4.00	4.00	1	1.25	0.06	372±6.12	−22.9±5.19	0.375±0.055
22	5.00	3	3	0.50	0.1	415±6.71	−21.5±4.20	0.453±0.058
23	5.00	3	3	2	0.02	422±4.24	−22.3±3.25	0.465±0.038
24	3.00	3	3	2	0.1	160±8.11	−21.0±2.31	0.250±0.053
25	4.00	4	2	1.25	0.06	334±6.24	−11.0±2.58	0.310±0.022
26	5.00	4	2	1.25	0.06	450±7.15	−21.2±7.80	0.550±0.021

[a]Stearic acid/lavender oil

[b]Span-80/tween-20

by Rotexmedica (Trittau, Germany) and Alfasan (Woerden-Holland), respectively. Topical Alpha® Ointment was purchased from Alpha Development Company (Iran). Deionized distilled water was freshly prepared. The analytical grade of all solvents and chemicals was applied for the experiments without further purification.

2.2 Animals

Thirty-six BALB/c male mice were obtained from Zabol University of Medical Sciences (Zabol, Iran) and all animal care and study protocols were directed in agreement with the rules and regulations applied by Zabol University of Medical Sciences Ethics Committee Acts and are according to the ARRIVE guidelines in reporting animal research. The mice were housed in separate polycarbonate cages at standard condition 22 ± 2 °C with a 12 h/12-h light–dark cycle.

Throughout the study, unlimited access to the laboratory regime and water ad libitum was permitted [28, 29]. Mice were randomly divided into six groups ($n=6$) as follows:

Group 1: receiving NLC- L_w- L_v (NLC with lawsone and lavender).
Group 2: receiving NLC- L_w (NLC with lawsone only).
Group 3: receiving NLC- L_v (NLC with lavender only).
Group 4: blank NLC (NLC without lawsone and lavender).
Group 5: negative control receiving distilled water.
Group 6: positive control receiving alpha® ointment.

2.3 Experimental Design and Statistical Analysis

Central composite design (CCD) was applied for optimization of RSM through Design-Expert software (Version

Table 2 Percent errors of obtained data for predicted and empirical values

Factor	Empirical data	Predicted data	Error%
Size	165	170.6	3.39
PDI	0.211	0.209	0.94
Zeta potential	− 24.3	− 25.2	3.70

DX7Trial) to discover the effect of the independent variables such as lawsone content, surfactant and lipid concentrations, feed ratio of the surfactants (Span® 80/tween-20), and lipid ratio (stearic acid/lavender oil) on the NLC features. The ranks of these factors are presented in Table 1 particle size, polydispersity index (PDI), and zeta potential (Z-P) were considered as dependent factors. Based on the obtained results, the optimized formulation was prepared and subjected to additional experiments [30].

2.4 Development of Lawsone-Loaded NLC

The lawsone-loaded NLCs were prepared using hot homogenization and ultrasound technique, as previously described [30]. The aqueous phase containing tween-20 and the lipid phase comprised of solid stearic acid and liquid lavender oil and also Span® 80 were prepared in separate tubes. The lipid phase was heated in a water bath at 75 °C until a clear solution was achieved. Lawsone was added to the lipid phase. Also, the liquid phase was heated on the water bath. Then, the hot aqueous surfactant was added to the lipid phase and dispersed by Ultra-Turrax T25 homogenizer (IKA T10, Germany) at 11,500 rpm for 6 min followed by 3 min sonication (70 s on and 30 s off cycles) using a probe sonicator (Bransonic, USA). To achieve a homogenous white suspension, the formulation was left at room temperature overnight to allow further formation of NLC. Blank NLCs were prepared in the same condition in the absence of lawsone [31].

2.5 Particle Size, Polydispersity Index, and Zeta Potential Measurement

The best formulation was characterized in terms of mean particle size, polydispersity index (PDI), and zeta potential (ZP). NLCs were diluted in deionized water (1:100), and dynamic light scattering (DLS) using a ZetaSizer (Nano-ZS; Malvern Instruments Ltd., UK) was determined at 25 °C at a 90° angle. The results (Table 2) are the means and standard deviations of three replications.

2.6 Fourier Transform-Infrared Spectroscopy (FTIR) Study

Fourier transform infrared (FT-IR) spectroscopy (IR PRESTIGE SHIMADZO) was used to detect variation in the molecular level of different formulations from 500 to 4000 cm^{-1}. NLC bearing lawsone and lavender and blank NLC (without lawsone) were freeze-dried to form a solid powder, then mixed and grounded with KBr and compressed under pressure for 10 min to give an appropriate disk.

2.7 Scanning Electron Microscopy (SEM)

The specimens were scanned with a scanning electron microscope (SEM: vp 1450 Leo, Germany) for visualization of morphology and structure. The samples were diluted in deionized water (1:15). Then, 20 μl of the sample was placed on a carbon-coated copper grid. It was dried after 30 s using a filter paper. Also, 20 μl of uranyl acetate 2% was placed on the grid and dried after 30 s. The prepared sample was observed under microscope and analyzed.

2.8 Entrapment Efficiency

To evaluate the entrapment efficiency (EE%) of lawsone in the formulation, the NLC- L_w- L_v was subjected to centrifugation for 30 min at 6000 rpm using Amicon Ultra-15-membrane (MWCO 10,000 Da). Briefly, 500 μl of the sample was transferred to the upper chamber of the filer. The supernatant was collected and after appropriate dilution with distilled water, the maximum absorption was determined at 410 nm using a UV–Vis spectrometer (CE1021, CECIL, England), and entrapment efficiency (EE%) was calculated based on Eq. (1):
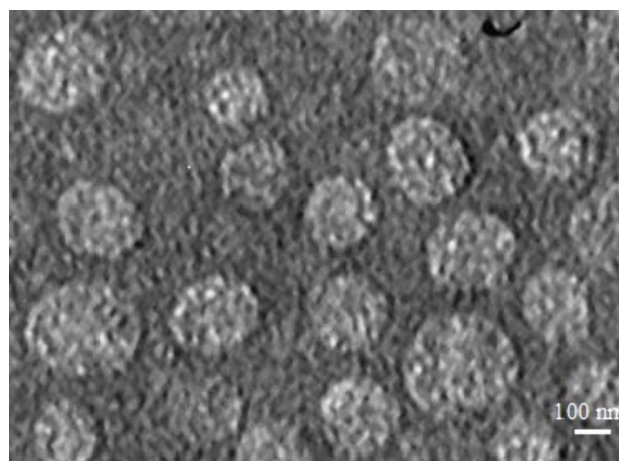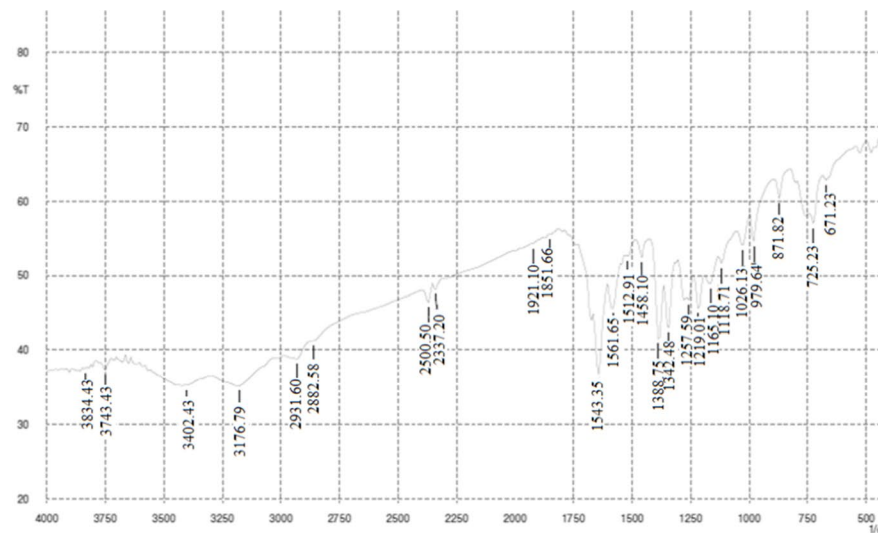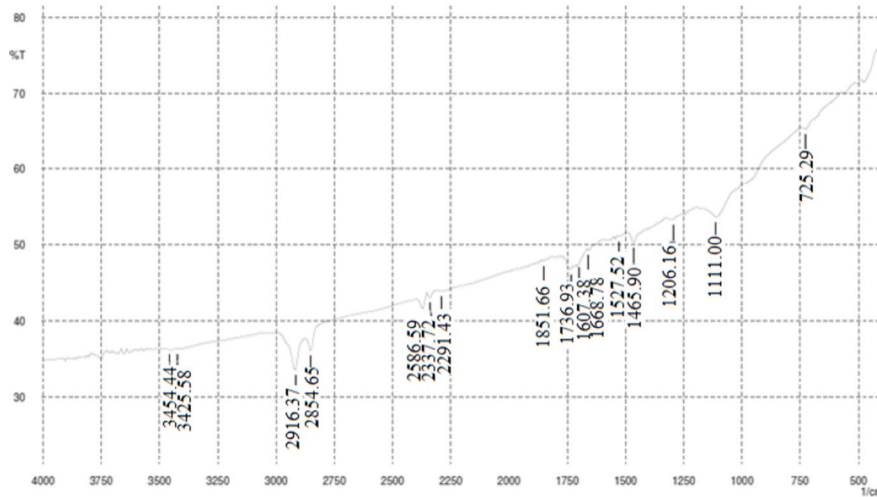

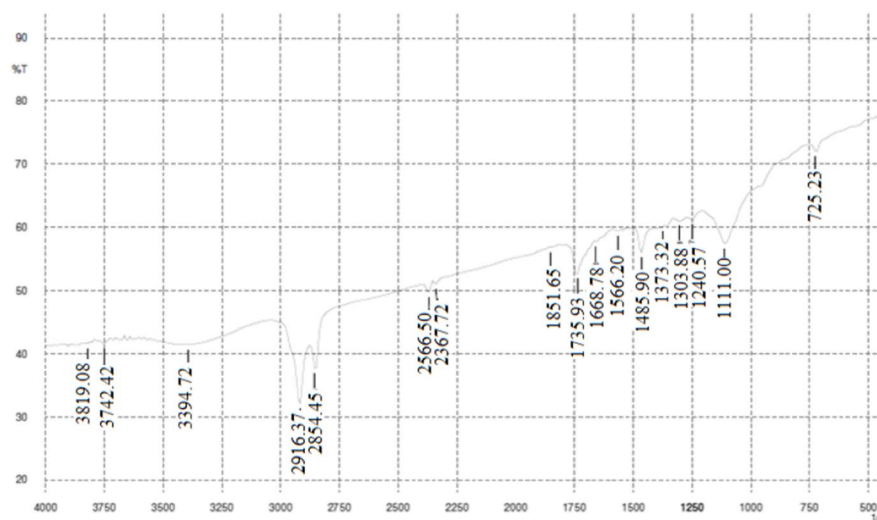**Fig. 1** Scanning electron microscopy image of NLC- L_w- L_v

A: FTIR spectra of Lawsone.

B: FTIR spectra of NLC- L$_w$- L$_v$.

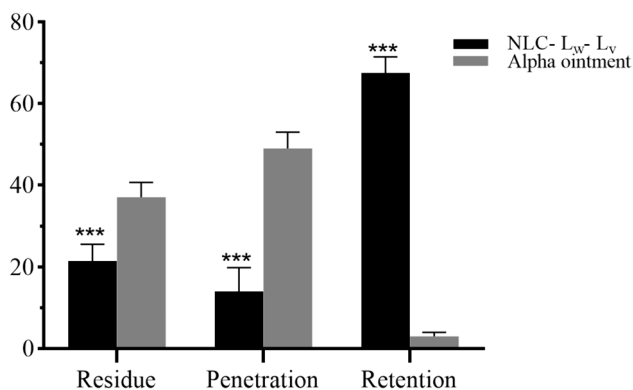**C:** FTIR spectra of blank NLC.

Fig. 3 The residue, penetration, and permeation rate of different Lawsone formulations (mean ± SD, $n = 3$). Asterisk (***) indicates $P < 0.001$. Data were compared using one-way analysis of variance (ANOVA) followed by Tukey's post hoc test

Fig. 4 Lawsone release of NLC- L_w -L_v and alpha ointment by Franz diffusion cells (mean ± SD, $n = 3$). Asterisk (***) indicates $P < 0.001$. Data were compared using one-way analysis of variance (ANOVA) followed by Tukey's post hoc test
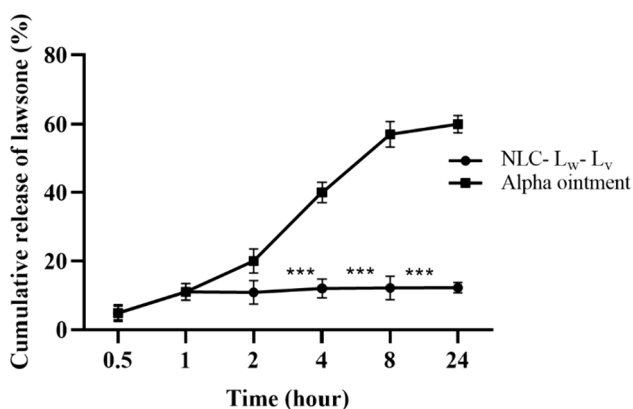
$$EE\% = \frac{total\ lawsone - free\ lawsone}{total\ lawsone} \times 100 \tag{1}$$

2.9 Ex Vivo Release Study

The standard Franz diffusion cells were applied for ex vivo release studies. Four independent Franz cells with a nominal capacity of receptor compartment of 25 ml and diffusion area of 1.54 cm^2 were selected. The dorsal skin of BALB/c male mice was shaved and placed in formalin for 1 h and cleaned through multiple washings with PBS. Circular pieces of skin were mounted onto the receptor chamber so that the stratum corneum confronted the donor compartment. Phosphate buffer solution and SLS 1% were used as

the receptor phase. The cells were arranged at 37 °C and the medium was retained at 32 °C using a water jacket with continuous stirring (200 rpm). An amount of 1 mg of different formulations, i.e., NLC- L_w- L_v, free lawsone, and alpha® ointment was applied to skin surface in the donor compartment. Alpha ointment is a conventional ointment of Lawsone. A 200 μl sample of the released medium was separated from the acceptor chamber and was exchanged with the same amount of isothermal PBS at different time points of 0.5, 1, 2, 4, 8, and 24 h. The obtained data were analyzed by using an analytical Knauer HPLC system with a k-2600 Knauer UV detector and a k-1001 Knauer pump.

To determine the retained values of formulations, the residue samples were removed from the surface of the skins and dissolved in 1 ml methanol-chloroform, filtered, and analyzed using HPLC. The retention value was determined by subtracting the extraction and residue values. Three similar experiments were repeated with every formulation [32].

3 Wound Healing Study

3.1 Excision Wound Creation

To immobilize the animals, anesthesia was induced by intraperitoneal injection of ketamine (60 mg/kg) and xylazine (7.5 mg/kg). The dorsal thoracic skin was shaved and sterilized with 70% ethanol and Povidone iodine solution before making a full-thickness skin excision of 3.5 mm^2 on the depilated skin of mice by a punch-biopsy tool. After creating the wounds, the mice were kept individually in the institutional animal facility.

3.1.1 Treatment

Mice were treated with different formulations once a day for a period of consecutive 14 days by the topical application so that the wounds were bandaged using a sterile gauze swab under anesthesia.

3.1.2 Wound Healing Assessment

Progressive variations in wound area were evaluated on days 0, 1, 2, 3, 5, 7, 9, 11, 13, and 14 and the size of wounds was measured by a caliper. Photographs were taken on the determined days after local anesthesia. A ruler was located adjacent to the wound site and photographed. The amount of wound contraction was calculated from the initial wound area and wound area after treatment using the following equation:

$$wound\ clousure\ rate = \frac{initial\ wound\ area - wound\ area\ after\ treatment}{initial\ wound\ area} \times 100 \tag{2}$$

3.1.3 Histopathological Analysis

On the 0th and 14th post-wounding days, the cross-sectional full-thickness skin samples were taken out for histopathological studies. For this purpose, six mice in each day were sacrificed with an overdose of CO_2 and the wound region and adjacent tissue were removed using dissecting scissors, scalpel, and forceps. The segments were fixed in 10% buffered formalin, treated, and blocked by paraffin. The prepared sections were stained using hematoxylin and eosin [9].

3.1.4 Effect of NLC- L_w- L_v on Oxidative Stress

Lipid peroxidation was measured by thiobarbituric acid reactive substance (TBARS). The test is based on the reaction of thiobarbituric acid and MDA that is produced in the oxidation process of polyunsaturated fatty acids. For the analysis, 2.0 ml of the homogenized sample was mixed with 1.0 ml of TBA buffer containing normal HCl 5.0%, TCA 15.0%, and TBA 3.0% and incubated in a water bath at 100 °C for 30 min. Then, samples were left at room temperature to cool down and then the absorbance was read at a wavelength of 532 nm. MDA solution was applied as standard to obtain calibration curves [33].

3.1.5 Statistical Analysis

The data were studied in three independent tests using SPSS version 21 and for each parameter mean values ± standard deviation were calculated. Data were compared using one-way analysis of variance (ANOVA) followed by Tukey's post hoc test. Statistical significance was acceptable when P-value was less than 0.05.

4 Results and Discussion

4.1 Optimization and Characterization of HESP-NLC (Particle Size, Polydispersity Index, and Zeta Potential Measurement)

CCD was developed to discover the optimal levels of selected independent parameters. Lawsone concentration, surfactant content, feed ratio of the surfactant (Span® 80/tween-20), lipid concentration, and feed ratio of lipids were chosen. Particle size, PDI, and zeta potential were selected as dependent factors. Mean particle size varied from 165 to 451 nm. The standard range of zeta potential was −11 to −24.3 mV and PDI ranged from 0.211 to 0.51.

The experimental results of size, PDI, and zeta potential for the best formulation were 165 ± 2.91 nm, 0.211, and −24.3 mV, respectively, while the corresponding predicted data were 170.6, 0.209, and −25.9 respectively. The data are presented in Table 1. The error percent was calculated from the below formula:

$$Error \% = \frac{experimental\ data - predicted\ data}{experimental\ data} \times 100 \quad (3)$$

The selected optimum formulation was applied for further assessments of the physico-chemical features and pharmacokinetic studies in a mouse model.

4.2 Scanning Electron Microscopy (SEM)

SEM image (Fig. 1) shows that NLC- L_w- L_v had fairly spherical shape and homogeneous size range. The particle diameter was about 100 nm that confirms the results of particle size analysis.

Table 3 The results of wound area on different days after treatment

Day	Negative control	Positive control	NLC- L_w -L_v	NLC- L_w	NLC- L_v	Blank	ANOVA
0	3.5 ± 0	3.5 ± 0	3.5 ± 0	3.5 ± 0	3.5 ± 0	3.5 ± 0	NS
1	3.35 ± 0.128	3.43 ± 0.118	3.28 ± 0.185	3.36 ± 0.021	3.42 ± 0.02	3.63 ± 0.051	NS
2	3.31 ± 0.148	$3.36 \pm 0.019*$	$3.15 \pm 0.011**$	3.1 ± 0.025	3.38 ± 0.175	3.3 ± 0.01	S
3	3.09 ± 0.031	$3.3 \pm 0.076*$	3.0 ± 0.094	2.97 ± 0.111	3.08 ± 0.151	3.11 ± 0.165	S
5	2.93 ± 0.116	$3.14 \pm 0.167*$	2.75 ± 0.072	$2.73 \pm 0.156*$	2.93 ± 0.185	3.0 ± 0.181	S
7	2.3 ± 0.148	2.5 ± 0.16	$2.06 \pm 0.182*$	$2.02 \pm 0.181*$	$1.97 \pm 0.187**$	2.11 ± 0.16	S
9	1.88 ± 0.176	1.75 ± 0.175	$1.33 \pm 0.181**$	$1.53 \pm 0.016**$	$0.97 \pm 0.037**$	1.62 ± 0.156	S
11	1.16 ± 0.138	1.36 ± 0.171	$0.45 \pm 0.154**$	$0.837 \pm 0.187**$	$0.65 \pm 0.058**$	1.05 ± 0.031	S
13	0.683 ± 0.138	$0.486 \pm 0.144*$	$0.25 \pm 0.034**$	$0.162 \pm 0.095**$	$0.16 \pm 0.03**$	$0.48 \pm 0.137*$	S
14	0.433 ± 0.171	0.396 ± 0.103	$0.0 \pm 0**$	$0.045 \pm 0.026**^\#$	$0.05 \pm 0.012**^\$$	$0.17 \pm 0.014**^\$$	S

NS insignificant difference, *S* significant difference

*Significant difference in comparison with negative control $P < 0.05$

**Significant difference in comparison with negative control $P < 0.05$

#Significant difference between NLC- L_w -L_v and NLC- L_w groups $P < 0.001$

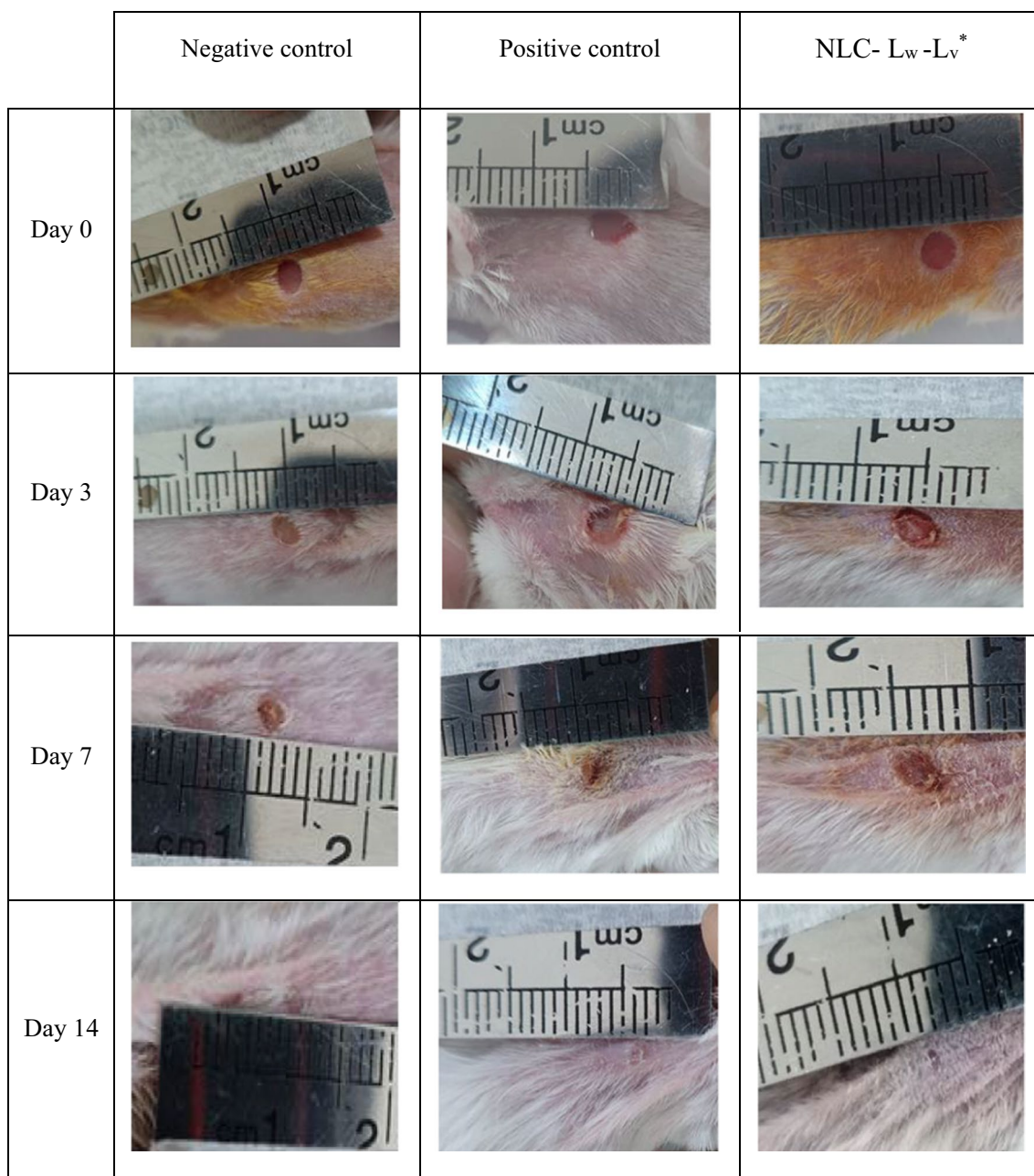$Significant difference in comparison with blank $P < 0.001$

Fig. 5 Macroscopic images of wound sites on different days in different treated groups during 14 days

4.3 Analysis of Fourier Transform Infrared (FTIR)

FT-IR technique was applied to confirm the interactions between lawsone and lipids during the preparation of NLC. The peak at 3402.43 cm^{-1} is assigned to O–H stretching in lawsone structure. The peaks at 2931.8, 1643.35, and 1388.75 cm^{-1} represent C-H stretching, C=O stretching, and C=C stretching, respectively. In the FT-IR spectrum of NLC- L_w- L_v, the bands related to lawsone are absent,

confirming the effective incorporation of lawsone into the lipids Fig. 2

4.4 Entrapment Efficiency

The amount of positioned drug within the lipid matrix is stated as entrapment efficiency. This value for the best formulation was 79.3 ± 2.9, showing that lawsone was entrapped in the NLC with a high loading efficacy. The
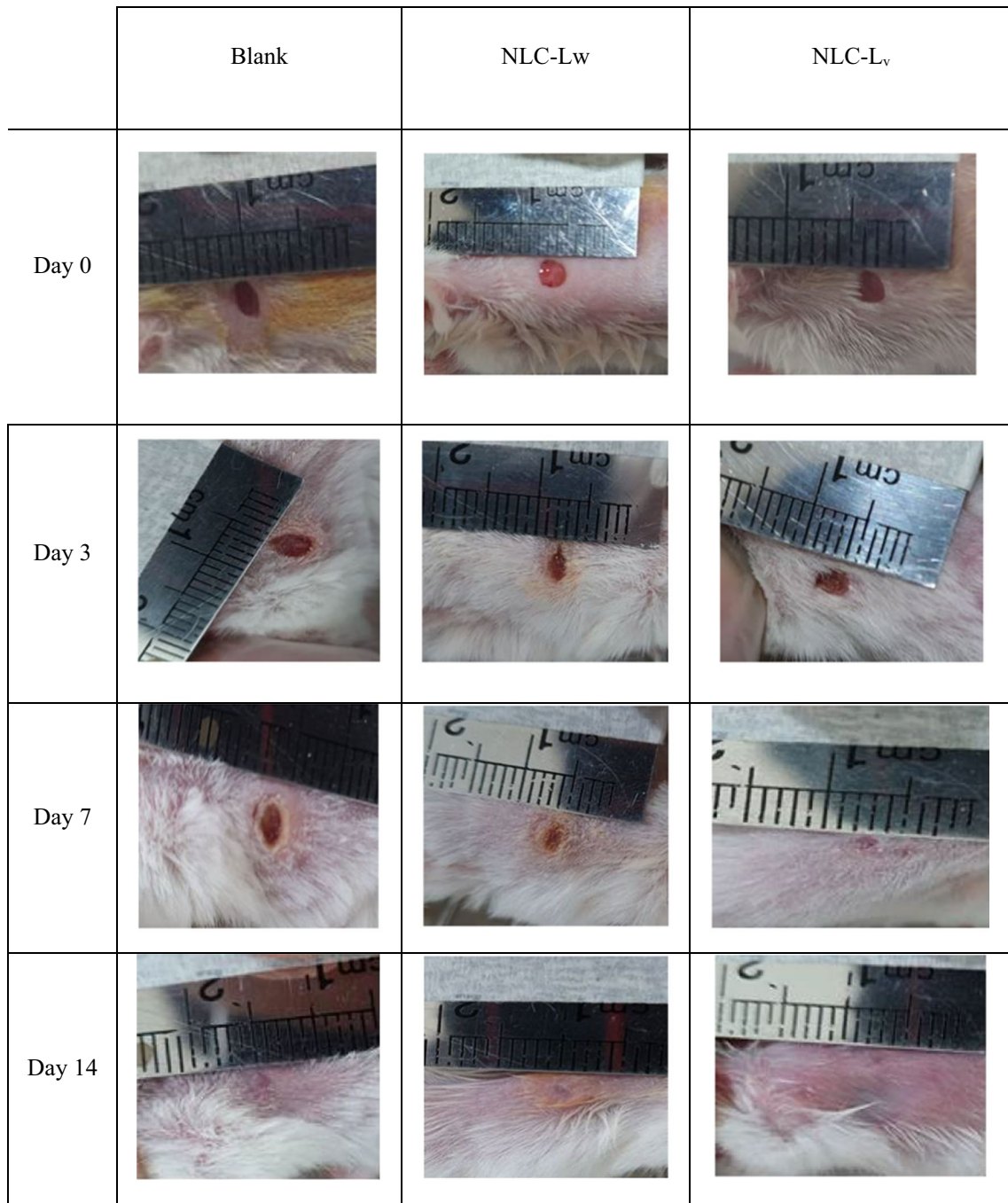
	Blank	NLC-Lw	NLC-L$_v$
Day 0			
Day 3			
Day 7			
Day 14			

Fig. 5 (continued)

standard deviation was also small, representing uniform encapsulation.

4.5 Ex Vivo Skin Penetration Test

The ability of prepared NLC- L_w- $L_v$to permeate skin was evaluated by a Franz diffusion cell. The rate of residue, penetration, and permeation of lawsone in the excised mouse dorsal skin 24 h after the experiment is shown in Fig. 3.

The retained amount of NLC- L_w- L_v in the skin was about 22.5 times higher than that of alpha ointment. In addition, lawsone in the NLC formulation was observed 5.2 times less than that of alpha ointment in the acceptor phase after 24 h. Also, the residue value was significantly lower in the case of NLC- L_w- L_v, indicating that the small-size nano
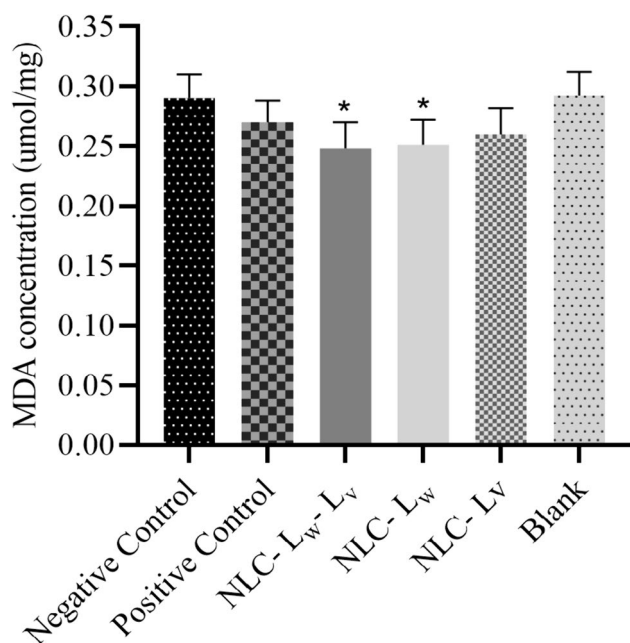
Fig. 6 MDA level for different groups on day 14. The error bars represent the mean $\pm$ SD from three replicate experiments. *$P < 0.05$. Data were compared using one-way analysis of variance (ANOVA) followed by Tukey's post hoc test

particles remained in the epidermis and do not diffuse into the acceptor phase. Briefly, lawson-NLC could entrap into the stratum corneum and accumulate in the dermis without diffusing to the acceptor compartment. These characteristics that result in the retention of nano formulation in the skin were efficient for dermal products owing to decreasing adverse effects from systemic circulation and targeted drug delivery [34].

4.6 Ex Vivo Drug Release and Kinetic Studies

In this study, the release pattern of NLC- L_w- L_v in comparison with alpha ointment was investigated. NLC- L_w- L_v exhibit a typically different release model in comparison with pure lawsone. A biphasic graph was observed for NLC- L_w- L_v, indicating a primary burst release pattern within 0.5 h followed by a controlled release over the remaining time for 24 h. As shown in Fig. 4, the mean value of drug release was significantly different for the tested formulations. Only 12.8% of lawsone was released from NLC- L_w- L_v, while in the case of alpha ointment (conventional lawsone ointment), the value was up to 60.0%.

The initial burst could be assigned to the amount of free adsorbed drug on the surface of NLC. In such circumstances, the molecules tend to depart from the formulation in an explosive manner. The plateau phase is the consequence of the slow diffusion of the drug from the lipid matrix that

depends on the homogeneous dispersion of the drug that is influenced by the drug character and entrapment model [9].

4.7 In Vivo Wound Healing Activity

To assess the effect of lawsone in lipid formulation on wound healing in comparison with alpha ointment, the progress of wound closure was followed at different time intervals after treatment. For this purpose, a circular excision was created on the dorsal skin of mice and wound area was measured. The results are presented in Table 3. The wound contraction rate on days 0th and 1st among different groups was insignificant ($P > 0.05$). On the second day, a significant difference in mean wound area was observed between NLC- L_w- L_v and negative control ($P < 0.01$). After 3 days, the healing rates among different treated groups were not statistically significant. NLC- L_w (NLC containing lawsone) group showed a significant difference from negative control on the 5th day ($P < 0.05$). At day 7, NLC- L_w, NLC- L_v (NLC containing lavender), and NLC- L_w- L_v (NLC containing lawsone and lavender) groups showed a significant healing rate compared with negative control ($P < 0.05$). The significance level of difference between the treated groups and negative control on days 9 and 11 was $P < 0.05$, on the 13th and 14th day, the healing performance compared to negative control was significant ($P < 0.05$). The difference between NLC- L_w- L_v group and NLC- L_w, NLC- L_v groups was significant and also the difference between NLC- L_w, NLC- L_v groups and blank was significant ($P < 0.001$).

The results of macroscopic wound contraction for different time intervals versus healing time are depicted in Fig. 5, which indicates that at the end of the experiment, almost the whole wound area was healed in NLC- L_w- L_v group, and wound size of zero was reported. In a previous research, Lakshmi et al. reported that lawsone 1% dermal gel stimulated wound healing rate of 99.2% after 16 days of treatment [35]. In this research, the proposed formulation promoted the healing process and the skin mended the initial structure after 14 days.

4.8 Lipid Peroxidation Analysis: Malondialdehyde (MDA) Measurement

Since the sources of vitamin E diminish in the patients with burn as a result of increasing lipid peroxidation, then the dermal application of free radical scavengers promotes the healing rate and prevents the tissue from oxidative damage. To evaluate the amount of lipid peroxidation, the MDA levels in the wounded skin tissue samples were assessed on post-wounded day 14 and the results are depicted in Fig. 6. The MDA level was significantly decreased in the

Fig. 7 a The swelling score of different treated groups. Data are shown as mean ± SD based on triplicate independent experiments. *$P < 0.05$, ** $P < 0.01$, ***$P < 0.001$. Data were compared using one-way analysis of variance (ANOVA) followed by Tukey's post hoc test. **b** The granulation score of different treated groups. Data are shown as mean ± SD based on triplicate independent experiments. *$P < 0.05$, ** $P < 0.01$, ***$P < 0.001$. Data were compared using one-way analysis of variance (ANOVA) followed by Tukey's post hoc test. **c** The fibrotic tissue formation of different treated groups. Data are shown as mean ± SD based on triplicate independent experiments. *$P < 0.05$, **$P < 0.01$, ***$P < 0.001$. Data were compared using one-way analysis of variance (ANOVA) followed by Tukey's post hoc test. **d** The re-epithelialization score of different treated groups. Data are shown as mean ± SD based on triplicate independent experiments. *$P < 0.05$, **$P < 0.01$, ***$P < 0.001$. Data were compared using one-way analysis of variance (ANOVA) followed by Tukey's post hoc test
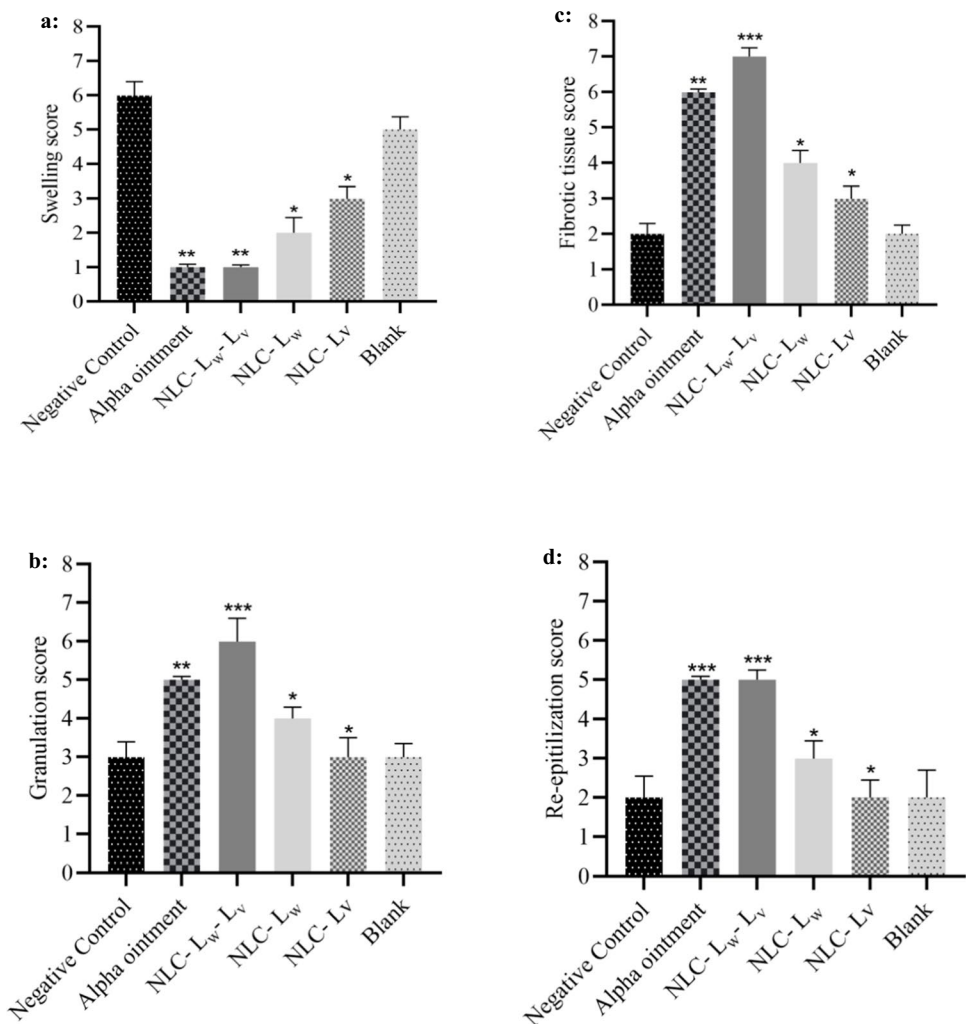
NLC- L_w- L_v and NLC- L_w groups compared with negative control ($P < 0.05$) [36, 37].

4.9 Histopathology and Healing Score

Hematoxylin and eosin (H&E) staining was used to evaluate microscopic wound healing parameters such as swelling, re-epithelialization, granulation, and fibrosis in wound tissue samples (Fig. 7a–d). On day 14, the sections were prepared and the results of microscopic observation were scored from zero to eight. The blank and negative control groups displayed a significant number of inflammatory cells while in the NLC- L_w- L_v group and alpha cream-treated group the inflammatory cells were different from negative control ($P < 0.01$). The results of NLC- L_w and NLC- L_v groups also showed a significant difference from negative control group ($P < 0.05$).

The degree of epithelial cell migration near the wound bed was greater in NLC- L_w- L_v and alpha cream groups than negative control ($P < 0.001$) and re-epithelialization seemed to be significant on the 14th day of treatment.

Moreover, the sections were assessed for the rate of granulation. Dermal application of NLC- L_w- L_v increased granulation tissue thickness even more than alpha ointment as positive control. Also, NLC- L_w and NLC- L_v groups showed a significant difference to negative control ($P < 0.05$). The other appraised parameter was fibrotic scars that are associate to type I collagen. As shown, the level of fibrotic scars in NLC- L_w- L_v group was higher than the reference drug alpha ointment. The NLC- L_w and NLC- L_v groups also showed a significant difference from negative control.

5 Conclusion

Nanostructured lipid carriers with small size and lipophilic character can easily interact with stratum corneum and allow better penetration into the skin, improve drug

accumulation and sustained release. In this research, to cover the orange red color and also improve the pharmacological effects of lawsone in wound healing, a formulation of lawsone incorporated NLC comprising stearic acid and lavender oil as lipids and using tween-20 (polysorbate) and Span® 80 as surfactants was synthesized by hot-homogenization and ultrasound technique. Morphological studies by SEM provided evidence of suitable dimensions (100 nm), zeta potential, and spherical shape. In the ex vivo permeation studies through the skin and into the skin, the formulation obviously improved the retention of lawsone as a result of forming a reservoir in the mouse skin and also reduced the residue and penetration value. Besides, the in vitro lipid peroxidation results showed that treatment with NLC- L_w- L_v successfully attenuates MDA level compared with negative control. The formulation was further studied for wound healing potential. In fact, NLC- L_w- L_v improved wound repair by decreasing inflammatory infiltration and swelling, induction of fibrotic tissues, dermal and epidermal renewal, and construction of well-structured skin.

In summary, the newly synthesized formulation could be used as a matrix carrier of lawsone, making a reservoir for long skin residence time, and therefore a preferred treatment for topical applications.

Author Contribution S. D.: conception of the work, conducting the study, revising the draft, approval of the final version of the manuscript, and agreed for all aspects of the work. A. T.: conception of the work, approval of the final version of the manuscript, and agreed for all aspects of the work. M. S.: data analysis, approval of the final version of the manuscript, and agreed for all aspects of the work. O. Sh.: data analysis, the drafting and revising the draft, approval of the final version of the manuscript, and agreed for all aspects of the work. J. Sh.: conception of the work, drafting and revising the draft, data analysis, approval of the final version of the manuscript, and agreed for all aspects of the work.

Data Availability The data are available on request.

Declarations

Informed consent None.

Ethics Approval and Consent to Participate Not applicable.

Consent for Publication Not applicable.

Conflict of Interest The authors declare that there are no conflicts of interest in this study.

Research Involving Humans and Animals Statement All animal experiments were authorized by the Ethics Committee Acts of Zabol University of Medical Sciences and conducted in accordance with their guidelines.

References

1. Flanagan, M. (2013). *Wound healing and skin integrity: Principles and practice*. John Wiley & Sons.
2. Eming, S. A., Martin, P., & Tomic-Canic, M. (2014). Wound repair and regeneration: Mechanisms, signaling, and translation. *Science Translational Medicine., 6*(265), 265sr6-sr6.
3. Sparks, H. D., Mandla, S., Vizely, K., Rosin, N., Radisic, M., & Biernaskie, J. (2022). Application of an instructive hydrogel accelerates re-epithelialization of xenografted human skin wounds. *Science and Reports, 12*(1), 14233.
4. Mohan, S., Syam, S., Abdelwahab, S. I., & Thangavel, N. (2018). An anti-inflammatory molecular mechanism of action of α-mangostin, the major xanthone from the pericarp of Garcinia mangostana: An in silico, in vitro and in vivo approach. *Food & function., 9*(7), 3860–3871.
5. Akbik, D., Ghadiri, M., Chrzanowski, W., & Rohanizadeh, R. (2014). Curcumin as a wound healing agent. *Life sciences., 116*(1), 1–7.
6. Panichayupakaranant, P., & Reanmongkol, W. (2002). Evaluation of chemical stability and skin irritation of lawsone methyl ether in oral base. *Pharmaceutical Biology, 40*(6), 429–432.
7. Charoensup, R., Duangyod, T., Palanuvej, C., & Ruangrungsi, N. (2017). Pharmacognostic specifications and lawsone content of Lawsonia inermis leaves. *Pharmacological Research, 9*(1), 60.
8. Barani, M., Mirzaei, M., Torkzadeh-Mahani, M., & Nematollahi, M. H. (2018). Lawsone-loaded niosome and its antitumor activity in MCF-7 breast cancer cell line: A nano-herbal treatment for cancer. *Daru, 26*, 11–17.
9. Adeli-Sardou, M., Yaghoobi, M. M., Torkzadeh-Mahani, M., & Dodel, M. (2019). Controlled release of lawsone from polycaprolactone/gelatin electrospun nano fibers for skin tissue regeneration. *International Journal of Biological Macromolecules, 124*, 478–491.
10. Patil, K. S. (2003). Wound healing potential of some active principles of Lawsonia alba Lam. leaves. *Indian journal of pharmaceutical sciences, 65*(4), 390.
11. Lakshmi, P., Thangellapalli, N., Chennuri, A., Prasanthi, D., & Veeresh, B. (2017). Wound healing activity of topical lawsone gel on rat model. *International Journal of Pharmaceutical Sciences and Research, 8*, 3162–3169.
12. Jridi, M., Sellimi, S., Lassoued, K. B., Beltaief, S., Souissi, N., Mora, L., et al. (2017). Wound healing activity of cuttlefish gelatin gels and films enriched by henna (Lawsonia inermis) extract. *Colloids and Surfaces A: Physicochemical and Engineering Aspects, 512*, 71–79.
13. FattahiBafghi, A., MahmoodzadehPournaki, A., & Hejazian, S. (2010). Immunosupressive effects survey of Lavandula spica L. extract on Cutaneous Leishmaniasis in BALB/c Mice. *Iranian Journal of Medicinal and Aromatic Plants Research, 25*(4), 540–6.
14. Kurkin, V., Lamrini, M., & Klochkov, S. (2008). Lavandoside from Lavandula spica flowers. *Chemistry of Natural Compounds, 44*(2), 169–170.
15. Silva, G. L., Luft, C., Lunardelli, A., Amaral, R. H., Melo, D. A., Donadio, M. V., et al. (2015). Antioxidant, analgesic and

anti-inflammatory effects of lavender essential oil. *Anais da Academia Brasileira de Ciências, 87*, 1397–408.

16. Samuelson, R., Lobl, M., Higgins, S., Clarey, D., & Wysong, A. (2020). The effects of lavender essential oil on wound healing: A review of the current evidence. *Journal of Alternative and Complementary Medicine, 26*(8), 680–690.

17. Khaliq, F. A., Raza, M., Hassan, S. U., Iqbal, J., Aslam, A., Aun, M., et al. (2018). Formulation, characterization and evaluation of in vivo wound healing potential of Lawsone ointment. *American Journal of Advanced Drug Delivery, 6*(01), 61–68.

18. Mori, H.-M., Kawanami, H., Kawahata, H., & Aoki, M. (2016). Wound healing potential of lavender oil by acceleration of granulation and wound contraction through induction of TGF-β in a rat model. *BMC Complementary and Alternative Medicine, 16*(1), 1–11.

19. Hartman, D., & Coetzee, J. (2002). Two US practitioners' experience of using essential oils for wound care. *Journal of Wound Care, 11*(8), 317–320.

20. Altaei, D. T. (2012). Topical lavender oil for the treatment of recurrent aphthous ulceration. *American Journal of Dentistry, 25*(1), 39–43.

21. Vakilian, K., Atarha, M., Bekhradi, R., & Chaman, R. (2011). Healing advantages of lavender essential oil during episiotomy recovery: A clinical trial. *Complementary Therapies in Clinical Practice, 17*(1), 50–53.

22. Sheikhan, F., Jahdi, F., Khoei, E. M., Shamsalizadeh, N., Sheikhan, M., & Haghani, H. (2012). Episiotomy pain relief: Use of Lavender oil essence in primiparous Iranian women. *Complementary Therapies in Clinical Practice, 18*(1), 66–70.

23. Mukherjee, S., Ray, S., & Thakur, R. (2009). Solid lipid nanoparticles: A modern formulation approach in drug delivery system. *Indian Journal of Pharmaceutical Sciences, 71*(4), 349.

24. Radtke, M., Souto, E. B., & Müller, R. H. (2005). Nanostructured lipid carriers: A novel generation of solid lipid drug carriers. *Pharmaceutical Technology Europe, 17*(4), 45–50.

25. Muller, H. R., Shegokar, R., & Keck, M. C. (2011). 20 years of lipid nanoparticles (SLN & NLC): Present state of development & industrial applications. *Current Drug Discovery Technologies, 8*(3), 207–27.

26. Pardeike, J., Hommoss, A., & Müller, R. H. (2009). Lipid nanoparticles (SLN, NLC) in cosmetic and pharmaceutical dermal products. *International Journal Of Pharmaceutics, 366*(1–2), 170–184.

27. Zsikó, S., Cutcher, K., Kovács, A., Budai-Szűcs, M., Gácsi, A., Baki, G., et al. (2019). Nanostructured lipid carrier gel for the dermal application of lidocaine: Comparison of skin penetration testing methods. *Pharmaceutics., 11*(7), 310.

28. James, O., & Victoria, I. A. (2010). Excision and incision wound healing potential of Saba florida (Benth) leaf extract in Rattus novergicus. *International Journal of Pharmacy & Biomedical Research, 1*(4), 101–107.

29. Irajirad, R., Ahmadi, A., Najafabad, B. K., Abed, Z., Sheervalilou, R., Khoei, S., et al. (2019). Combined thermo-chemotherapy of cancer using 1 MHz ultrasound waves and a cisplatin-loaded sonosensitizing nanoplatform: An in vivo study. *Cancer Chemotherapy and Pharmacology, 84*, 1315–1321.

30. Shahraki, O., Shayganpour, M., Hashemzaei, M., & Daneshmand, S. (2023). Solid lipid nanoparticles (SLNs), the potential novel vehicle for enhanced in vivo efficacy of hesperidin as an anti-inflammatory agent. *Bioorganic Chemistry, 131*, 106333.

31. Shiehzadeh, F., Mir, E., Raeesi, S., Daneshmand, S., & Shahraki, J. (2022). Nanostructured lipid carriers (NLCs) composed of argan oil, the potential novel vehicle for caffeine delivery to stratum corneum and hair follicles. *Nanomedicine Journal, 9*(1), 87–94.

32. Venter, J. P., Müller, D. G., du Plessis, J., & Goosen, C. (2001). A comparative study of an in situ adapted diffusion cell and an in vitro Franz diffusion cell method for transdermal absorption of doxylamine. *European Journal of Pharmaceutical Sciences, 13*(2), 169–177.

33. Hassani, S., Yaghoubi, H., Khosrokhavar, R., Jafarian, I., Mashayekhi, V., Hosseini, M.-J., et al. (2015). Mechanistic view for toxic effects of arsenic on isolated rat kidney and brain mitochondria. *Biologia, 70*(5), 683–689.

34. Daneshmand, S., Jaafari, M. R., Movaffagh, J., Malaekeh-Nikouei, B., Iranshahi, M., Moghaddam, A. S., et al. (2018). Preparation, characterization, and optimization of aurapten-loaded solid lipid nanoparticles as a natural anti-inflammatory agent: In vivo and in vitro evaluations. *Colloids and Surfaces B, 164*, 332–339.

35. Pereira, L. X., Silva, H. K. C., Longatti, T. R., Silva, P. P., Oliveira, C. D. L., Proietti, ABd. F. C., et al. (2017). Achyrocline alata potentiates repair of skin full thickness excision in mice. *Journal Of Tissue Viability, 26*(4), 289–99.

36. Mingjian, Z., Qifang, W., Lanxing, G., Hong, J., & Zongyin, W. (1992). Comparative observation of the changes in serum lipid peroxides influenced by the supplementation of vitamin E in burn patients and healthy controls. *Burns, 18*(1), 19–21.

37. Farmoudeh, A., Akbari, J., Saeedi, M., Ghasemi, M., Asemi, N., & Nokhodchi, A. (2020). Methylene blue-loaded niosome: Preparation, physicochemical characterization, and in vivo wound healing assessment. *Drug Delivery and Translational Research, 10*, 1428–1441.